Influence of the twist angle on the plasticity of the GaAs compliant substrates realized by wafer bonding

2002 J. Phys.: Condens. Matter 14 12967

(http://iopscience.iop.org/0953-8984/14/48/339)

INSTITUTE OF PHYSICS PUBLISHING JOURNAL OF PHYSICS: CONDENSED MATTER

J. Phys.: Condens. Matter **14** (2002) 12967–12974 PII: S0953-8984(02)53984-9

Influence of the twist angle on the plasticity of the GaAs compliant substrates realized by wafer bonding

G Patriarche[1] **and E Le Bourhis**[2]

[1] Laboratoire de Photonique et de Nanostructures, UPR 20 CNRS, Route de Nozay, 91460 Marcoussis, France
[2] Université de Poitiers, Laboratoire de Métallurgie Physique, UMR 6630 CNRS, SP2MI-Téléport 2, Boulevard Marie et Pierre Curie, BP 30179, 86962 Chasseneuil Cedex, France

E-mail: gilles.patriarche@lpn.cnrs.fr

Received 27 September 2002
Published 22 November 2002
Online at stacks.iop.org/JPhysCM/14/12967

Abstract

We have investigated the structure and mechanical behaviour of twist-bonded GaAs compliant substrates. For a twist angle lower than 15°, the bonded interface was observed to contain a dense network of pure screw dislocations. For a larger twist angle, no dislocations were observed at the bonding interface. The mechanical behaviours of these compliant substructures were investigated using nanoindentation and the results were compared to those obtained for standard bulk GaAs. It appears that the nature of the interface has a great influence on the mechanical properties of these compliant substrates.

(Some figures in this article are in colour only in the electronic version)

1. Introduction

The fabrication of electronic and optoelectronic devices requires semiconductor materials of high structural quality. Their active region is often a complex structure involving heteroepitaxial layers grown on a substrate. Above a critical thickness of the layer (which decreases rapidly with increasing misfit), the epitaxial layers relax plastically through the introduction of misfit dislocations at the interface. Unfortunately, this relaxation process also generates a large density of threading dislocations extending between the interface and the surface. Not only are these dislocations unnecessary to relaxation, they also deleteriously affect the optical and electrical properties of the structure. The various procedures tried in order to eliminate them in standard epitaxy have so far remained insufficiently efficient.

The use of compliant substructures was proposed to overcome this problem [1]. The misfit between the substrates must be accommodated by elastic or plastic deformation in a zone localized near the interface. Fabrication of compliant substrates involves the use of a thin compliant layer bonded to a bulk substrate with a large twist disorientation (several degrees to several tens of degrees [2, 3]).

To quantify the plastic relaxation enhancement that could be obtained with these new structures, we have used the nanoindentation technique, which is adapted to the sub-micron scales encountered in compliant substructures [4–8].

2. Experimental details

2.1. Fabrication of the compliant substructures

The compliant substructures were obtained by first bonding two non-intentionally doped GaAs substrates twisted through a large angle θ (between 6° and 45°) with respect to each other around their common normal. The bonded surfaces, slightly above 1 cm^2, were non-intentionally disoriented (001) planes. The bonding temperature and time were about 600 °C and one hour, respectively. After bonding, one side of the assembly was thinned, first down to a few tens of micrometres by mechanical polishing, and then down to a few nanometres by chemical etching, using etch-stop layers previously deposited on the wafer. After this procedure, the compliant substructure is made of a thin layer bonded to the host substrate, the interface being located at about 20 nm depth.

2.2. Nanoindentation tests

The tests were performed at room temperature in the force-control mode of the machine. The indenter was a Berkovitch diamond pyramid applied on the (001) plane. Samples were oriented so that one side of the Berkovitch indenter was aligned along a ⟨110⟩ crystallographic direction. Indentation arrays were made for subsequent relocalization in the transmission electron microscope (TEM) samples. Large indentations were used as markers. The maximum load was varied between 0.15 and 2 mN.

2.3. Transmission electron microscopy of thin foils

TEM plan views of the interface of the compliant substrates and of the plastic zone generated by the indenter have been obtained for samples mechanically and chemically thinned with a bromine–methanol solution. In the case of the indented samples only the undeformed side of the samples (the back) was thinned.

3. Structures of the different compliant substrates

3.1. Compliant substrates based on a low-angle twist boundary

At least up to $\theta = 16°$, the TEM plan-view images of the twist-bonded interface under weak-beam (WB) conditions (usually $(\boldsymbol{g}, 4\boldsymbol{g})$) showed a square dislocation network (observed only for low twist by Ejeckam *et al* [2]). Figure 1 shows the $\boldsymbol{g} = [220]$ diffraction condition where only one half of the dislocations are observed. The lines are separated by 2.02 nm and are nearly parallel to $\boldsymbol{g}$. In fact they are parallel to the bisector of the ⟨110⟩ directions of the two crystals closest to each other. Using the orthogonal $\boldsymbol{g} = [\bar{2}20]$ diffraction condition, the other half of the dislocations were observed. The square network is constituted of two sets of pure screw dislocations with Burgers vectors $b = (a/2)\langle 110\rangle$ lying in the interface.

The spacing D between screw dislocations accommodating for a twist angle θ can be calculated from

$$D = \frac{|b|}{2\sin(\theta/2)}.$$

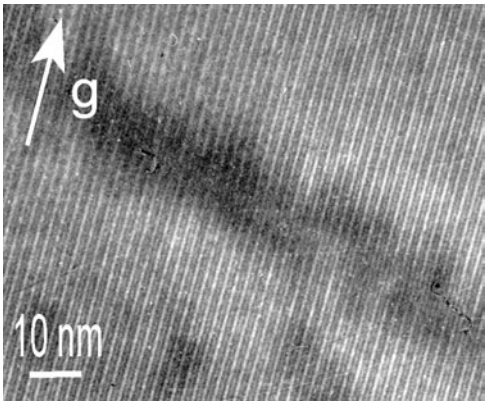

Figure 1. A plan-view image of the $\theta = 11^\circ$ twist-bonded compliant substrate under the $\boldsymbol{g} = [220]$ WB condition. One set of screw dislocations (of the first network) parallel to $\boldsymbol{g}$ is observed. The image is centred on the intersection of one dislocation of the second network with the first network.

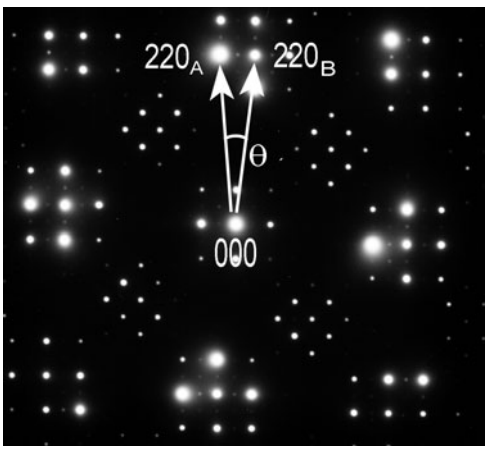

Figure 2. A (001) diffraction pattern of a thin foil of $\theta = 11^\circ$ twist-bonded compliant substrate in plan view. The index (A or B) refers to the substrate or the compliant layer. The weak extra spots between the main spots are associated with the diffraction of the network of the screw dislocations.

For a twist angle $\theta = 11^\circ$ (measured directly in figure 2 from the electron diffraction pattern) we find a distance of about 2.04 nm, which is very close to our former measurements [9].

A second network was also observed. It is a single set of roughly parallel dislocations which appeared in the strong-beam images as broken lines with a spacing varying between samples (usually between 100 and 160 nm). Although they produce no contrast, these dislocations appear in the WB images when they interact with the screw dislocations of the first network. The latter are all shifted by half their spacing upon crossing a line of the second set. This shows that the dislocations of the second network have Burgers vectors of the $(a/2)\langle 101\rangle$ type not lying in the interface. Similar observations have already been made in the cases of Si/Si twist bonding [10] and of GaAs/InP heteroepitaxial bonding [3]. This second set accommodates the slight disorientation of the bonded surfaces from nominal (001) planes.

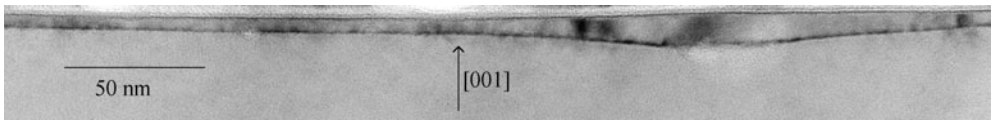

Figure 3. A TEM cross-sectional view of the compliant structure showing the layer on top of the substrate. The common [001] direction normal to the substrate and to the layer is also shown. Before assembling, the layer was twisted by about $\theta = 37°$ around the common normal.

3.2. Compliant substrates based on a large-angle twist boundary

Figure 3 is a TEM cross-sectional view of the second compliant substrate showing the thin compliant layer bonded on top of the substrate. The [001] direction normal to the structure is common to the layer and to the substrate. Before bonding, the layer was twisted by a large angle θ. Using the TEM diffraction patterns obtained in plan view, θ was determined to be about 35°. This means that 2° separates the actual boundary from an ideal $\Sigma 5$ boundary. This difference is expected to increase the energy E of the boundary as the $E(\theta)$ curve is very steep around $\theta = 37°$ [11].

On the other hand, the cross-sectional view showed great variations of the compliant layer thickness (figure 3). This is attributed to the lateral displacement of material during the heat treatment that is used to bond the structure. One effect of this treatment is to increase dramatically the roughness of the interface. This roughness is expected to induce friction between the compliant layer and the substrate underneath and therefore to affect the free-standing performance of the compliant layer. It should be noted that no interfacial layer (oxide or amorphous) could be detected in the vicinity of the interface. Furthermore, no dislocations were observed at the interface contrary to what was reported for compliant layers bonded with low twist angle [9, 12]. This result agrees very well with predictions made by Jesser *et al* [13].

4. Plastic behaviour of the compliant substrates

4.1. Compliant substrates based on a low-angle twist boundary

The indentation curves of low-angle twist compliant substrate and bulk GaAs are presented in figure 4. In the loading portion of the indenting curve both reversible and non-reversible deformation occurred. During the unloading, the reversible (elastic) deformation was recovered leaving a residual deformation. The maximum depths measured on the compliant substrate were found very close to those measured on bulk GaAs. In fact the two materials showed similar hardnesses.

All the loading portions of the indentation curves in the compliant substrates were continuous like the one presented in figure 4. No 'pop-in' event occurred contrary to what was observed for bulk GaAs. Such pop-in events are expected to appear in materials with very poor initial defect density such as bulk GaAs. In the compliant substructure, dislocation nucleation is expected to happen more easily because of the high density of defects located at the interface (section 3.1). This interface introduces a high density of dislocation nucleation sites.

Figure 5 shows a TEM plan view of the surface of the compliant substrate after indentation. For the maximum loads used here (ranging between 0.5 and 1.7 mN), a plastic zone was always observed as expected from the indentation curves. No cracks were observed in or around these plastic zones, in contrast with what is generally reported for bulk GaAs for high indenting loads [14]. The dislocation density was very high in the plastic zones (figure 5).

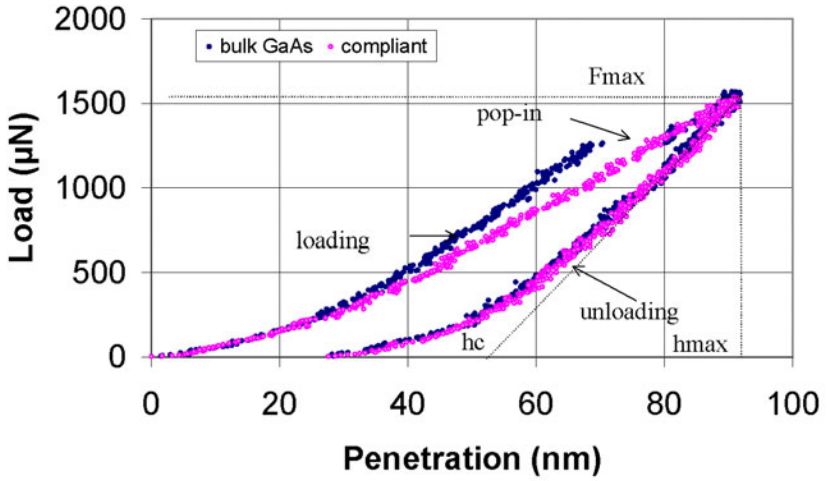

Figure 4. Loading and unloading curves of a Berkovitch indenter in a low-angle twisted compliant substrate and in (001) bulk GaAs at room temperature. During loading, a 'pop-in' event is observed in bulk GaAs for a critical load of about 1.3 mN.

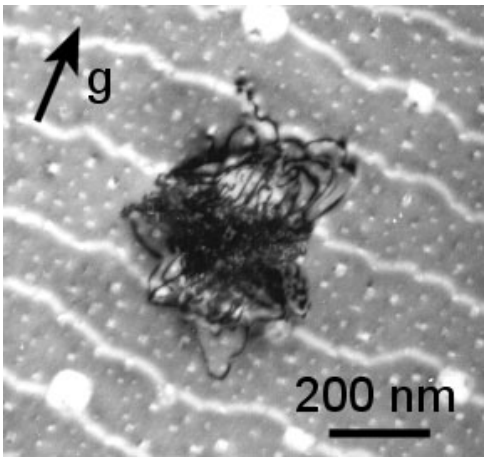

Figure 5. A transmission electron micrograph of a $\theta = 7°$ twisted GaAs compliant substrate indented at room temperature under a maximum load of 0.5 mN. The second set of dislocations is visible under $\boldsymbol{g} = [\bar{2}20]$. Their lines are almost parallel to [110].

Only the edges of the plastic zone showed individual dislocation lines. The extension of such dislocations increased with increasing load on the indenter. Under about 5 mN load, we observed the beginning of rosette arms that are generally observed under higher loads [11, 12].

To determine the flow stress of bulk and compliant GaAs, we measured the plastic zone size as a function of the maximum load. By TEM, we determined the diameter of the projection of the plastic zone on the (001) plane considering only the dense region of the plastic zone. The diameter was averaged along the two orthogonal ⟨110⟩ directions parallel to the surface. In figure 6, the plastic zone radius c is plotted as a function of the square root of the maximum load F_{max} determined from the indentation curves (figure 4). We plotted about 40 points corresponding to 20 different indentation tests obtained for each material.

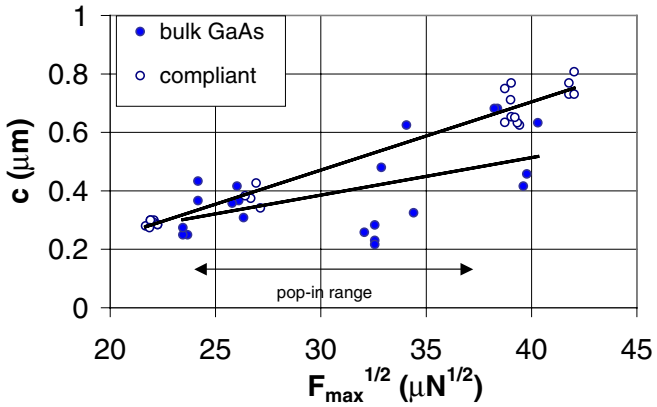

Figure 6. Plastic zone radius as a function of the square root of the maximum load for the $\theta = 7°$ twisted GaAs compliant substrates. The maximum load was measured on the loading curves. The plastic zone radius was measured by TEM.

A large scatter in the measurements was obtained for bulk GaAs. This scatter is attributed to the pop-in events. The pop-in range (between 0.6 and 1.3 mN) covers almost all of the load range investigated here. Nonetheless, it can be observed that the plastic zone radius is larger in the compliant substrates than in bulk GaAs. The compliant substrates were deformed continuously when pop-ins appeared in bulk GaAs. Therefore, the material flow under the indenter is more gradual and efficient in the first case.

From figure 6, the variation between c and $\sqrt{F_{max}}$ can be fitted. Starting with the data for the compliant substrate (which show less scatter) a linear variation can be obtained and this is shown in the figure. Extrapolation of the data yields a threshold load F_{th} of about 0.1 mN for the compliant structure. This value is an estimate of the load necessary for plastic deformation to initiate in the compliant structure.

As a first approximation, we used the Johnson equation $c = \sqrt{3F_{max}/(2\pi Y)}$ [15] with c-values determined under the highest maximum load used in this study (F_{max} about 2 mN). In fact, we assumed that in that case $F_{th} \ll F_{max}$ was satisfied. This let us determine the flow stress values of 1.5 and 2.8 GPa for the compliant substrates and bulk GaAs respectively. Both flow stress values are of the same order of magnitude as those determined by compression experiments (<1 GPa at room temperature [16, 17]). As already mentioned in a previous paper [18], the discrepancy between compression and indentation experiments can be attributed to the difference in strain rates. Further compression testing at room temperature requires confining pressure and/or predeformation to avoid fracture of the samples. This procedure makes the experiment and determination of flow stress very difficult below the brittle–ductile transition and only a few values have been reported in the literature [16, 17].

4.2. Compliant substrates based on a large-angle twist boundary

Figure 7 shows loading and unloading curves of the indenter in the so-called Σ5 twist-bonded compliant structure as well as the curves for bulk GaAs under very low maximum loads (0.25 and 0.2 mN respectively). The loading and unloading curves superimpose for the compliant structure while they slightly separate for the bulk substrate. In the first case, only reversible (elastic) deformation is generated under the indenter. This was carefully checked by TEM. Observations of the indent site under 0.25 mN showed no plastic zone in the Σ5 substructure, while under 0.2 mN a plastic zone was observed in the bulk substrate.

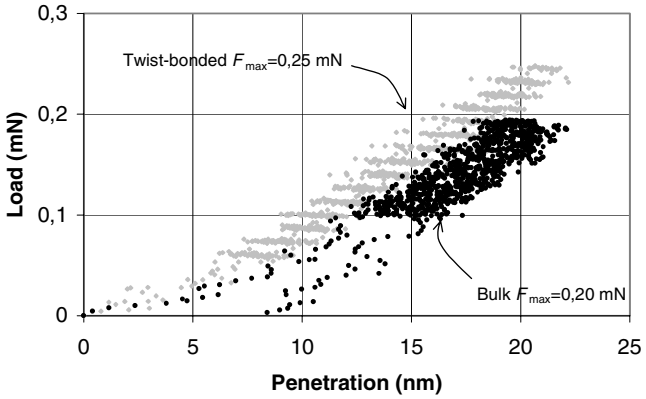

Figure 7. Loading and unloading curves of a Berkovitch indenter at room temperature in the Σ5 compliant substrates (under 0.25 mN) and in bulk (001) GaAs (under 0.2 mN).

When loading the compliant substrate under higher maximum load, the loading curves showed a discontinuity (pop-in) for a critical load F_c of about 0.4 mN and the unloading curve separated from the loading curve. The TEM plan view showed a plastic zone at the indent site. Pop-in corresponds to an abrupt plastic flow generated by a strong dislocation activity (nucleation and propagation). We observed here two different behaviours before pop-in. In bulk GaAs some dislocations are nucleated in the sample before pop-in occurs, as confirmed by the TEM observations of the indent site under 0.2 mN. When the load reaches the value at pop-in (about 0.4 mN), dislocation propagation initiates and penetration of the indenter increases abruptly. In contrast, for loads below about 0.4 mN the Σ5 compliant substrate is deformed only elastically and no plastic zone is generated, as confirmed by TEM. Once the indenting load reaches the critical value F_c, dislocation nucleation and propagation occur at the same level of stress and pop-in is observed. These results are strong experimental confirmations of the free-standing behaviour of the compliant layer. Nonetheless, we did not observe a larger plastic onset shift in the structure designed with a Σ5 boundary than in a 45° twist-bonded compliant structure [19]. In fact, complex phenomena have to be considered to understand the free-standing behaviour. Among related factors, the energy of the boundary as well as the roughness of the interface are believed to be pertinent parameters. However, their respective contributions are complex, as revealed by our experimental results.

5. Conclusions

We have studied the structure and the mechanical behaviour of twist-bonded compliant substrates. Plastic deformation could be generated in the compliant GaAs substrates as well as in a GaAs bulk reference at room temperature under a Berkovitch indenter submitted to low loads ranging between 0.15 and 2 mN.

The TEM study shows that the compliant substrates based on a low-angle twist boundary (<16°) have a bonded interface constituted by a dense network of screw dislocations. Larger plastic zones were observed in the compliant substrates than in bulk GaAs. Assuming the relation of Johnson [15], the flow stress of the compliant substructure was found to be about 30% lower than that of bulk GaAs.

In compliant substrates based on a large-angle twist boundary, no dislocation is present at the bonded interface. Further, we observed a wide shift of the plastic threshold for the Σ5

compliant structure. The twist angle (close to 37°) was chosen because of the low energy of the $\Sigma 5$ coincident boundary. Plastic threshold shift is a strong experimental confirmation that free-standing behaviour can be engineered using such twist-bonded substrates [20].

References

[1] Lo Y H 1991 *Appl. Phys. Lett.* **59** 2311
[2] Ejeckam F E, Lo Y H, Subramanian S, Hou H Q and Hammons B E 1997 *Appl. Phys. Lett.* **70** 1685
[3] Patriarche G, Jeannès F, Oudar J L and Glas F 1997 *J. Appl. Phys.* **82** 4892
[4] Newey D, Wilkins M A and Pollock H M 1982 *J. Phys. E: Sci. Instrum.* **15** 119
[5] Pethica J B, Hutchings R and Oliver W C 1983 *Phil. Mag.* A **48** 593
[6] Doerner M F and Nix W D 1986 *J. Mater. Res.* **1** 601
[7] Oliver W C and Pharr G M 1992 *J. Mater. Res.* **7** 1564
[8] Dargenton J C and Woirgard J 1996 *J. Physique* III **6** 1247
[9] Patriarche G, Mériadec C, Le Roux G, Deparis C, Sagnes I, Harmand J-C and Glas F 2000 *Appl. Surf. Sci.* **164** 15
[10] Benamara M, Rocher A, Laporte A, Sarrabayrousse G, Lescouzères L, PeyreLavigne A, Fnaiech M and Claverie A 1995 *Mater. Res. Soc. Symp. Proc.* **378** 863
[11] Priester L 1980 *Rev. Phys. Appl.* **15** 789
[12] Patriarche G and Le Bourhis E 2000 *Phil. Mag.* A **80** 2899
[13] Jesser W A, Van der Merwe J H and Stoop P M 1999 *J. Appl. Phys.* **85** 2129
[14] Warren P D, Pirouz P and Roberts S G 1984 *Phil. Mag.* A **50** L23
[15] Johnson K L 1985 *Contact Mechanics* (Cambridge: Cambridge University Press)
[16] Boivin P, Rabier J and Garem H 1990 *Phil. Mag.* A **61** 619
[17] Suzuki T, Yasutomi T, Tokuaka T and Yonenaga I 1999 *Phys. Status Solidi* a **71** 47
[18] Le Bourhis E and Patriarche G 1999 *Phil. Mag. Lett.* **79** 805
[19] Patriarche G and Le Bourhis E 2001 *Appl. Surf. Sci.* **178** 134
[20] Le Bourhis E and Patriarche G 2001 *Phil. Mag. Lett.* **81** 813